JACS
JOURNAL OF THE AMERICAN CHEMICAL SOCIETY

Communication

pubs.acs.org/JACS

Ni−C−N Nanosheets as Catalyst for Hydrogen Evolution Reaction

Jie Yin,[†] Qiaohui Fan,[§] Yuxuan Li,[†] Fangyi Cheng,[¶] Panpan Zhou,[†] Pinxian Xi,*[,†] and Shouheng Sun*[,‡]

[†]Key Laboratory of Nonferrous Metal Chemistry and Resources Utilization of Gansu Province, State Key Laboratory of Applied Organic Chemistry, and The Research Center of Biomedical Nanotechnology, Lanzhou University, Lanzhou 730000, P. R. China

[‡]Department of Chemistry, Brown University, Providence, Rhode Island 02912, United States

[§]Key Laboratory of Petroleum Resources, Gansu Province/Key Laboratory of Petroleum Resources Research, Institute of Geology and Geophysics, Chinese Academy of Sciences, Lanzhou 730000, P. R. China

[¶]Key Laboratory of Advanced Energy Materials Chemistry (Ministry of Education), Nankai University, Tianjin 300071, P. R. China

Supporting Information

ABSTRACT: We report a facile nitrogenation/exfoliation process to prepare hybrid Ni−C−N nanosheets. These nanosheets are <2 nm thin, chemically stable, and metallically conductive. They serve as a robust catalyst for the hydrogen evolution reaction in 0.5 M H_2SO_4, or 1.0 M KOH or 1.0 M PBS (pH = 7). For example, they catalyze the hydrogen evolution reaction in 0.5 M H_2SO_4 at an onset potential of 34.7 mV, an overpotential of 60.9 mV (at j = 10 mA cm^{-2}) and with remarkable long-term stability (~10% current drop after 70 h testing period). They are promising as a non-Pt catalyst for practical hydrogen evolution reaction.

Electrocatalytic water splitting is considered a green and sustainable way of producing hydrogen (H_2) as a promising alternative to fossil fuels for future energy needs.[1] Platinum (Pt) has been the most active catalyst studied for this splitting, especially for the electrochemical reduction of proton to H_2, which is commonly referred to as hydrogen evolution reaction (HER), with high current density at low overpotentials.[2] However, Pt does have its limitation in serving as the catalyst for large-scale H_2 production due to its poor abundance and high cost.[3] To solve this problem, numerous efforts have been devoted to developing non-Pt catalysts, including tungsten-,[4] molybdenum-,[5] cobalt-,[6] iron-,[7] and nickel-based[8] catalysts, for the HER in acidic media.[9] Considering the inevitable proton concentration change during the HER process, the ideal catalyst should perform equally well in different pH solutions so that the water splitting process can be more energy-efficient.[10] Unfortunately, this has not been an easy goal to achieve.

Recent studies indicate that transition metal carbides (TMCs) have a low energy barrier for hydrogen adsorption,[11] and its density of states (DOS) near the Fermi level resemble some of the noble metals.[12] This leads to the attention to nickel carbide (NiC), which is chemically stable in solutions of a broad pH range, as a promising new noble-metal-free catalyst for the HER.[13] Further studies show that the activity of NiC can be improved by doping another element, such as nitrogen (N), due to the favorable tuning of the electronic structure of Ni,[14] and the electron conductivity of NiC may be enhanced by reducing the catalyst dimension from bulk to 2D sheet structure.[15] Herein, we take advantage of the easy formation of nickel nitride (Ni_3N)[16] and synthesize a new form of hybrid Ni−C−N nanosheets (NSs) containing NiC and Ni_3N. The ultrathin (<2 nm) Ni−C−N NSs show intrinsic metallic conductivity and function as a highly active and durable elecrtocatalyst for the HER in 0.5 M H_2SO_4, or 1.0 M KOH or 1.0 M PBS (pH = 7).

A two-step process (see details in the Supporting Information (SI)) was developed to synthesize the Ni−C−N NSs. First, the bulk Ni−C−N was obtained by annealing Ni−polyoxometalate metal−organic framework (Ni-POMMOF)[17] in a NH_3 atmosphere at 380 °C for 3 h and washed with 3.0 M HCl. Then, the bulk Ni−C−N was exfoliated to Ni−C−N NSs through a combination of sonication and wet chemical exfoliation process in formamide.[18] The NiC NSs and Ni_3N NSs were also synthesized (SI) and used as controls. Figure 1a shows the X-ray diffraction (XRD) patterns of the Ni−C−N NSs, NiC NSs, and Ni_3N NSs. The diffraction peaks of the NiC NSs indicate the presence of the cubic NiC structure with a

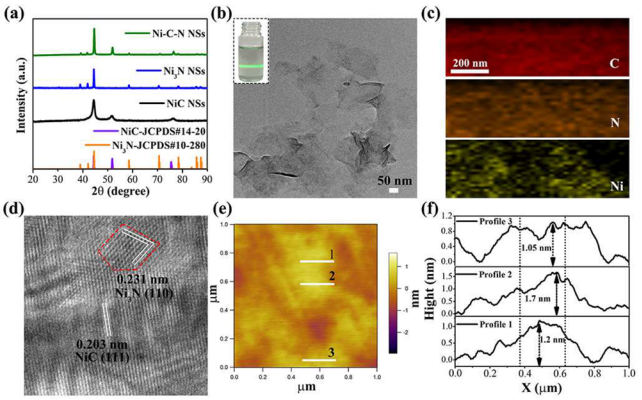

Figure 1. (a) XRD patterns of the hybrid Ni−C−N NSs, NiC NSs, and Ni_3N NSs. (b) TEM image of the Ni−C−N NSs. Inset: Tyndall effect of the colloidal Ni−C−N NSs in water. (c) Elemental mapping of a selected area of the Ni−C−N NS. (d) High-resolution TEM image of a selected area of the Ni−C−N NS. (e) AFM image and (f) height profiles of the exfoliated Ni−C−N NS. The profiles 1, 2, and 3 correspond to the numbered lines in panel e, respectively.

Received: September 6, 2016
Published: October 24, 2016

DOI: 10.1021/jacs.6b09351
J. Am. Chem. Soc. 2016, 138, 14546−14549

space group of $Fm\bar{3}m$ (JCPDS No. 14-20; $a = b = c = 3.539$ Å). The peaks of the Ni_3N NSs are from the hexagonal Ni_3N with a space group of $P6_322$ (JCPDS No.10-280; $a = b = 4.621$ Å; $c = 4.304$ Å). The peaks of the Ni−C−N NSs contain both NiC and Ni_3N peaks, suggesting the formation of the NiC−Ni_3N hybrid structure. The NS structure of Ni−C−N is further confirmed by the transmission electron microscopy (TEM) analysis (Figure 1b) and elemental mapping of the selected sheets (Figure 1c). The near transparency image of the sheets in Figure 1b is an indicative of the formation of the thin structure.[19] The elemental mapping in Figure 1c shows the uniform distribution of C, N, and Ni across the sheet area. The HRTEM image of a selected area of the NS (Figure 1d) shows lattice fringe spacing of 0.203 and 0.231 nm, corresponding to the interplanar distance of (111) and (110) of NiC and Ni_3N, respectively. Atomic force microscopy (AFM) was used to evaluate the thickness of the Ni−C−N NSs (Figure 1e,f). The heights of the Ni−C−N NSs measured across lines 1−3 range from 1.05 to 1.70 nm. The NS structures of NiC and Ni_3N were also characterized by TEM and HRTEM (Figure S1).

The electron conductivity of the NS films was measured via the common 4-probe method and the room temperature resistance of the 1 mm thick film was calculated to be 0.4 Ohm (SI) that is close to 0.1 Ohm obtained from a copper slice. The NS film also had a temperature-dependent resistance behavior (Figure 2a). These indicate that the Ni−C−N NSs are

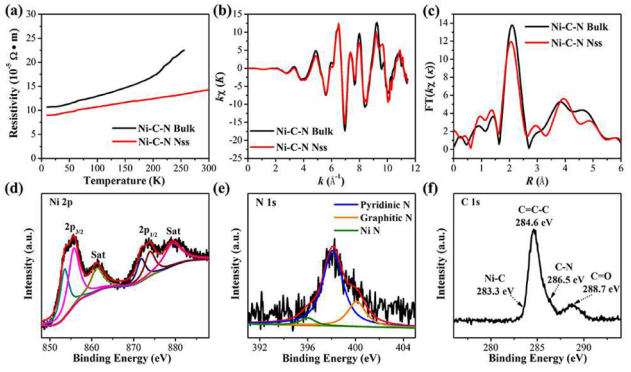

Figure 2. (a) Temperature-dependent electrical resistivity of the Ni−C−N NSs and Ni−C−N bulk. (b) Ni K-edge EXAFS oscillation and (c) the corresponding Fourier transforms. XPS spectra of (d) Ni 2p, (e) N 1s, and (f) C 1s of the Ni−C−N NSs.

metallic.[20] Extended X-ray absorption fine structure spectroscopy (EXAFS) of the Ni−C−N at the Ni K-edge (Figure 2b) shows that the Ni−C−N NS sample presents an oscillation similar to the bulk Ni−C−N but with a slightly different $k_3\chi(k)$ function. The corresponding Fourier Transforms (FTs) (Figure 2c) present two peaks in the range of 1−3 Å. The first one ranging from 1.0 to1.4 Å correspond to Ni−C/N pair (the scattering of C or N cannot be distinguished), and the second one in the range of 1.4−3 Å is due to the scattering pair of Ni−Ni. Intensity of the Ni−C/N pair in the Ni−C−N NS structure is stronger than that from the bulk Ni−C−N, but this is reversed when the Ni−Ni peaks from two different samples are compared. Further fitting (Table S1) confirms that the local atomic arrangement in the NSs is indeed different from that in the bulk Ni−C−N and the Ni−C−N NS is structurally more disordered than the bulk one.[21] X-ray photoelectron spectra (XPS) of the Ni−C−N NSs (Figure 2d) show two spin−orbit doublets of Ni 2p and two shakeup satellites (denoted as "Sat."), which are characteristic of Ni^{2+} and Ni^{3+}.[22a] The N 1s spectrum (Figure 2e) is the sum of three different types of nitrogen species in pyridinic N, graphitic N, and N−Ni.[10a] Four different C species are also identified from the C 1s spectrum (Figure 2f), in which the peak at 283.3 eV is related to NiC.[22b]

The catalytic performance of the Ni−C−N NSs for the HER was evaluated by using the linear scan voltammogram (LSV). For comparison, the electrocatalytic activity of the commercially available benchmark Pt/C catalyst (20 wt % Pt on carbon black from Premetek. Co, mass loading of 0.2 mg cm^{-2}), Ni-POMMOF, NiC NSs, and Ni_3N NSs were also measured. Figure 3a shows the LSV curves of the HER in 0.5 M H_2SO_4

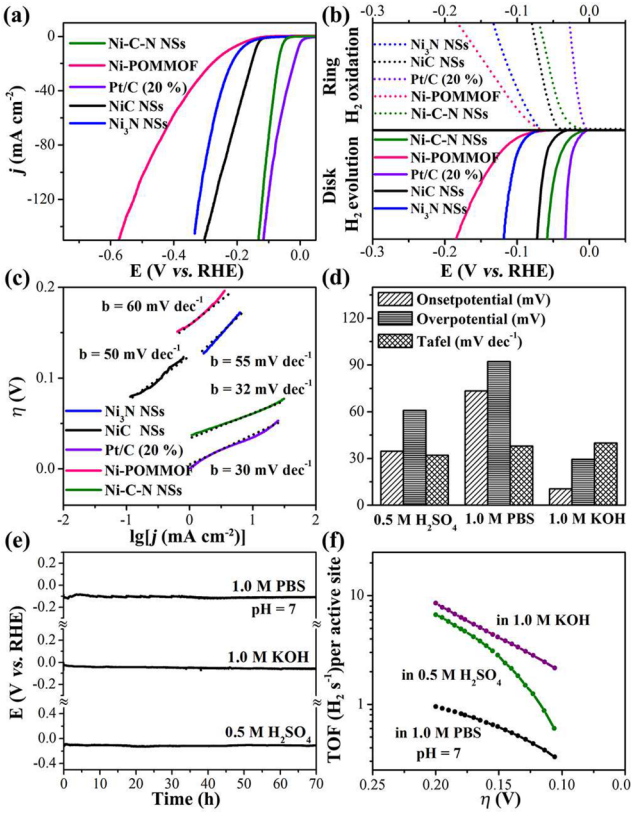

Figure 3. (a) LSV HER curves for the Ni−C−N NSs, Ni-POMMOF, NiC NSs, Ni_3N NSs, and Pt/C (20%) in 0.5 M H_2SO_4 (scan rate of 2 mV s^{-1}). (b) RRDE measurements of H_2 evolution on different catalyst-modified electrodes. The Pt-ring electrode was maintained at 0.7 V for the oxidation of the H_2 that was evolving on the disk electrode. (c) Tafel plots of different catalysts in 0.5 M H_2SO_4. (d) Summary of onset potential, Tafel slope and overpotential at j = 10 mA cm^{-2} for the HER catalyzed by Ni−C−N NSs in an acid (0.5 M H_2SO_4), or neutral (1.0 M PBS), or basic (1.0 M KOH) solution. (e) Chronopotentiometric curves of the Ni−C−N NSs with the constant current density of 10 mA cm^{-2}. (f) TOF plots of the Ni−C−N NSs in different pH conditions.

catalyzed by the Ni−C−N NSs, Ni-POMMOF, NiC NSs, Ni_3N NSs, and Pt/C catalysts. The Ni−C−N NS catalyst has an onset potential of 34.7 mV, close to the value from the Pt/C and much smaller than the values from Ni-POMMOF (129 mV), NiC (105 mV), and Ni_3N (110 mV). The overpotential (η) at j = 10 mA cm^{-2} for the Ni−C−N is 60.9 mV, much lower than that observed on the NiC (141 mV) and Ni_3N (190 mV) (Figure S2). The rotating ring disk electrode (RRDE) test[23] confirms that H_2 is produced selectively by all catalysts

DOI: 10.1021/jacs.6b09351
J. Am. Chem. Soc. 2016, 138, 14546−14549

(Figure 3b). Figure 3c displays the Tafel plots (log $j \sim \eta$) of the HER. The HER on the Pt/C with a Tafel slope of 30 mV dec^{-1} follows the known Tafel mechanism ($H_{ads} + H_{ads} \rightarrow H_2\uparrow$).[24] The Ni−C−N has a very similar Tafel slope of 32 mV dec^{-1}, suggesting that the HER on this catalyst is also dominated by the Tafel mechanism. The exchange current density (j_0) of the Ni−C−N was calculated to be 1.36×10^{-5} A cm^{-2} (Figure S3). This value is close to that obtained from the most active porous 1T-MoS_2 NS catalyst (1.58×10^{-5} A cm^{-2}).[25] The Ni−C−N catalyzed HER at 0.4 V has a nearly quantitative faradaic efficiency after a period of 60 min, confirming that the reduction current is from the HER (Figure S4). The Ni−C−N NS catalyst performs slight higher activity in 1.0 M KOH, but less so in 1.0 M phosphate buffered saline (PBS, pH = 7) (Figure 3d), and its catalysis behavior is similar to the Pt/C but much better than the controls (Figures S5 and S6) and many other non-noble-metal HER catalysts reported (Table S2). Our data show that in 1 M KOH, the Ni−C−N NSs becomes the most efficient catalyst to promote the H_2 formation via Heyrovsky process $H_2O + M{-}H_{ad} \rightleftharpoons M + H_2 + OH^-$.[24]

The stability of the Ni−C−N NS catalyst was evaluated by time-dependent potential change in 0.5 M H_2SO_4, 1.0 M PBS, and 1.0 M KOH (Figure 3e). In these tests, the current drop after a 70 h testing period is ∼10% and the morphology and structure of the catalyst is well-preserved (Figure S7). Assuming all Ni's on the NS surface are active and are accessible to the electrolyte, we estimated that the Ni−C−N has $\sim 1.26 \times 10^{17}$ sites cm^{-2}. We could calculate the catalytic turnover frequency (TOF) of the HER in different solutions (Figure 3f and SI). The TOF of the Ni−C−N NSs catalyst is 6.67, 8.52, and 0.95 s^{-1} at η = 200 mV in 0.5 M H_2SO_4, 1.0 M KOH and 1.0 M PBS respectively, much better than any of those obtained from other known catalysts (Table S3).

To confirm that Ni-sites are indeed active for the HER, we studied thiocyanate ion (SCN^-) effect on the HER activity. Different from the study in PBS (pH = 7) where the number of active sites can be examined by CV,[26] when performing the test in an acid solution, SCN^- is known to poison the metal-sites.[27] In our test, once 10 mM SCN^- was introduced in 0.5 M H_2SO_4, the j values decrease significantly from 196.6 to 77.3 mA cm^{-2} at η = 150 mV (Figure 4a), inferring that 61% of Ni-sites are blocked by the SCN^- ions. In the same test condition, much more Ni-sites on the bulk Ni−C−N, NiC, and Ni_3N surfaces are blocked (Figure S8). XPS analysis of the Ni−C−N NSs (Figure 4b) shows that the Ni−C−N NSs structure has the weaker Ni 2p binding energy than either the NiC NSs or the Ni_3N NSs structure. It confirms that the hybrid formation of NiC and Ni_3N renders the Ni-sites prone to attacking by an electrophile, i.e., the Ni-sites in the Ni−C−N NSs structure become more active as the catalyst for HER.

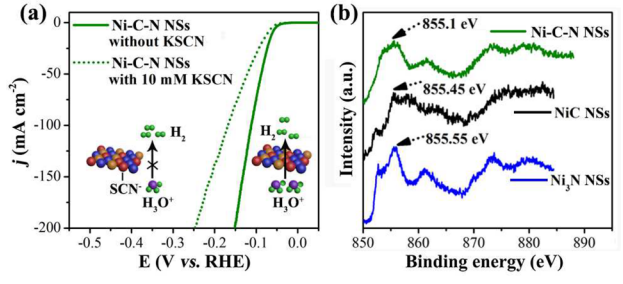

Figure 4. (a) LSV HER curves of the Ni−C−N NSs with or without 10 mM KSCN in 0.5 M H_2SO_4. Inset: illustrations of Ni-centers blocked by the SCN^- ions. (b) XPS spectra of Ni 2p for the Ni−C−N NSs, NiC NSs, and Ni_3N NSs.

In summary, starting with a Ni−polyoxometalate metal−organic framework (Ni-POMMOF) and using the common nitrogenization/sonication/exfoliation method, we have prepared the hybrid Ni−C−N NSs that are <2 nm thin and chemically stable. The Ni−C−N NSs show the metallic characters and can serve as a new kind of robust catalyst for the HER in 0.5 M H_2SO_4, or 1.0 M KOH, or 1.0 M PBS (pH = 7). The catalytic behavior of the Ni−C−N NSs is similar to that of the common Pt catalyst and it can work well in all pH values for more than 70 h without obvious current drop. Our work demonstrates that it is indeed possible to hybridize NiC with Ni_3N to enhance HER activity and stability to a level that is comparable to Pt. Judging from the overall catalytic performance, we can conclude that our Ni−C−N NS catalyst is one of the most active non-Pt catalysts ever reported. The concept of hybridization of NiC with Ni_3N to enhance NS catalysis is certainly not limited to Ni−C−N, but should be extended to other metal carbides as well, providing a promising new approach to M−C−N hybrid NSs for important functional materials and catalytic applications.

■ ASSOCIATED CONTENT

Supporting Information

The Supporting Information is available free of charge on the ACS Publications website at DOI: 10.1021/jacs.6b09351.

Experimental details, Figures S1−S8, and Tables S1−S3 (PDF)

■ AUTHOR INFORMATION

Corresponding Authors

*P.X. xipx@lzu.edu.cn

*S.S. ssun@brown.edu

Notes

The authors declare no competing financial interest.

■ ACKNOWLEDGMENTS

The work was supported by the National Natural Science Foundation of China (No. 21571089, 51571125, 41573128, 21601179) and the Fundamental Research Funds for the Central Universities (lzujbky-2016-k02 and lzujbky-2016-38). We also thank the staff at the BL14W1 station of the Shanghai Synchrotron Radiation Facility (SSRF) for EXAFS measurements and data analysis.

■ REFERENCES

(1) (a) Dresselhaus, M. S.; Thomas, I. L. *Nature* **2001**, *414*, 332−337. (b) Turner, J. A. *Science* **2004**, *305*, 972−974.

(2) Stamenkovic, V. R.; Mun, B. S.; Arenz, M.; Mayrhofer, K. J. J.; Lucas, C. A.; Wang, G.; Ross, P. N.; Markovic, N. M. *Nat. Mater.* **2007**, *6*, 241−247.

(3) McKone, J. R.; Warren, E. L.; Bierman, M. J.; Boettcher, S. W.; Brunschwig, B. S.; Lewis, N. S.; Gray, H. B. *Energy Environ. Sci.* **2011**, *4*, 3573−3583.

(4) (a) Wu, R.; Zhang, J.; Shi, Y.; Liu, D.; Zhang, B. *J. Am. Chem. Soc.* **2015**, *137*, 6983−6986. (b) Yan, H.; Tian, C.; Wang, L.; Wu, A.; Meng, M.; Zhao, L.; Fu, H. *Angew. Chem., Int. Ed.* **2015**, *54*, 6325−6329. (c) Voiry, D.; Yamaguchi, H.; Li, J.; Silva, R.; Alves, D. C. B.; Fujita, T.; Chen, M.; Asefa, T.; Shenoy, V. B.; Eda, G.; Chhowalla, M. *Nat. Mater.* **2013**, *12*, 850−855.

DOI: 10.1021/jacs.6b09351
J. Am. Chem. Soc. 2016, 138, 14546−14549

(5) (a) Lukowski, M. A.; Daniel, A. S.; Meng, F.; Forticaux, A.; Li, L.; Jin, S. *J. Am. Chem. Soc.* **2013**, *135*, 10274−10277. (b) Wang, S.; Ge, H.; Sun, S.; Zhang, J.; Liu, F.; Wen, X.; Yu, X.; Wang, L.; Zhang, Y.; Xu, H.; Neuefeind, J. C.; Qin, Z.; Chen, C.; Jin, C.; Li, Y.; He, D.; Zhao, D. *J. Am. Chem. Soc.* **2015**, *137*, 4815−4822. (c) Youn, D. H.; Han, S.; Kim, J. Y.; Kim, J. Y.; Park, H.; Choi, S. H.; Lee, J. S. *ACS Nano* **2014**, *8*, 5164−5173. (d) Wu, H. B.; Xia, B. Y.; Yu, L.; Yu, X.-Y.; Lou, X. W. *Nat. Commun.* **2015**, *6*, 6512−6519. (e) McEnaney, J. M.; Crompton, J. C.; Callejas, J. F.; Popczun, E. J.; Biacchi, A. J.; Lewis, N. S.; Schaak, R. E. *Chem. Mater.* **2014**, *26*, 4826−4831.

(6) (a) Jin, H.; Wang, J.; Su, D.; Wei, Z.; Pang, Z.; Wang, Y. *J. Am. Chem. Soc.* **2015**, *137*, 2688−2694. (b) Kong, D.; Wang, H.; Lu, Z.; Cui, Y. *J. Am. Chem. Soc.* **2014**, *136*, 4897−4900. (c) Popczun, E. J.; Read, C. G.; Roske, C. W.; Lewis, N. S.; Schaak, R. E. *Angew. Chem., Int. Ed.* **2014**, *53*, 5427−5430.

(7) Long, X.; Li, G.; Wang, Z.; Zhu, H.; Zhang, T.; Xiao, S.; Guo, W.; Yang, S. *J. Am. Chem. Soc.* **2015**, *137*, 11900−11903.

(8) Popczun, E. J.; McKone, J. R.; Read, C. G.; Biacchi, A. J.; Wiltrout, A. M.; Lewis, N. S.; Schaak, R. E. *J. Am. Chem. Soc.* **2013**, *135*, 9267−9270.

(9) (a) Tang, Y.-J.; Gao, M.-R.; Liu, C.-H.; Li, S.-L.; Jiang, H.-L.; Lan, Y.-Q.; Han, M.; Yu, S.-H. *Angew. Chem., Int. Ed.* **2015**, *54*, 12928−12932. (b) Wang, Z.-L.; Hao, X.-F.; Jiang, Z.; Sun, X.-P.; Xu, D.; Wang, J.; Zhong, H.-X.; Meng, F.-L.; Zhang, X.-B. *J. Am. Chem. Soc.* **2015**, *137*, 15070−15073.

(10) (a) Wang, S.; Wang, J.; Zhu, M.; Bao, X.; Xiao, B.; Su, D.; Li, H.; Wang, Y. *J. Am. Chem. Soc.* **2015**, *137*, 15753−15759. (b) Huang, Z.-F.; Song, J.; Li, K.; Tahir, M.; Wang, Y.-T.; Pan, L.; Wang, L.; Zhang, X.; Zou, J.-J. *J. Am. Chem. Soc.* **2016**, *138*, 1359−1365.

(11) (a) Ma, R.; Zhou, Y.; Chen, Y.; Li, P.; Liu, Q.; Wang, J. *Angew. Chem., Int. Ed.* **2015**, *54*, 14723−14727. (b) Ramaswamy, N.; Tylus, U.; Jia, Q.; Mukerjee, S. *J. Am. Chem. Soc.* **2013**, *135*, 15443−15449.

(12) Dong, S.; Chen, X.; Zhang, X.; Cui, G. *Coord. Chem. Rev.* **2013**, *257*, 1946−1956.

(13) (a) Lee, J. S. Metal Carbides. *Encyclopedia of Catalysis*; John Wiley & Sons: Hoboken, NJ, 2010. (b) Schwarz, K. *Crit. Rev. Solid State Mater. Sci.* **1987**, *13*, 211−257.

(14) (a) Zhao, Y.; Kamiya, K.; Hashimoto, K.; Nakanishi, S. *J. Am. Chem. Soc.* **2015**, *137*, 110−113. (b) Choi, C. H.; Park, S. H.; Woo, S. I. *ACS Nano* **2012**, *6*, 7084−7091. (c) Nistor, R. A.; Newns, D. M.; Martyna, G. J. *ACS Nano* **2011**, *5*, 3096−3103.

(15) (a) Xu, K.; Chen, P.; Li, X.; Tong, Y.; Ding, H.; Wu, X.; Chu, W.; Peng, Z.; Wu, C.; Xie, Y. *J. Am. Chem. Soc.* **2015**, *137*, 4119−4125. (b) Xie, J.; Zhang, J.; Li, S.; Grote, F.; Zhang, X.; Zhang, H.; Wang, R.; Lei, Y.; Pan, B.; Xie, Y. *J. Am. Chem. Soc.* **2013**, *135*, 17881−17888. (c) Chen, W.-F.; Muckerman, J. T.; Fujita, E. *Chem. Commun.* **2013**, *49*, 8896−8909.

(16) Gajbhiye, N. S.; Ningthoujam, R. S.; Weissmüller, J. *Phys. Status Solidi* **2002**, *189*, 691−695.

(17) Li, B. K.; Olson, D. H.; Lee, J. Y.; Bi, W.; Wu, K.; Yuen, T.; Xu, Q.; Li, J. *Adv. Funct. Mater.* **2008**, *18*, 2205−2214.

(18) Feng, J.; Peng, L. L.; Wu, C. Z.; Sun, X.; Hu, S. L.; Lin, C. W.; Dai, J.; Yang, J. L.; Xie, Y. *Adv. Mater.* **2012**, *24*, 1969−1974.

(19) Song, F.; Hu, X. *J. Am. Chem. Soc.* **2014**, *136*, 16481−16484.

(20) (a) Wu, Z.; Hao, Z.; Ying, P.; Li, C.; Xin, Q. *J. Phys. Chem. B* **2000**, *104*, 12275−12281. (b) Schlatter, J. C.; Oyama, S. T.; Metcalfe, J. E., III; Lambert, J. M. *Ind. Eng. Chem. Res.* **1988**, *27*, 1648−1653. (c) Oyama, S. T. *Catal. Today* **1992**, *15*, 179−200. (d) Cardona, C. M.; Elliott, B.; Echegoyen, L. *J. Am. Chem. Soc.* **2006**, *128*, 6480−6485.

(21) Kibsgaard, J.; Chen, Z.; Reinecke, B. N.; Jaramillo, T. F. *Nat. Mater.* **2012**, *11*, 963−969.

(22) (a) Yin, J.; Zhou, P.; An, L.; Huang, L.; Shao, C.; Wang, J.; Liu, H.; Xi, P. *Nanoscale* **2016**, *8*, 1390−1400. (b) Benayad, A.; Li, X.-S. *J. Phys. Chem. C* **2013**, *117*, 4727−4733.

(23) (a) Le Goff, A.; Artero, V.; Jousselme, B.; Tran, P. D.; Guillet, N.; Métayé, R.; Fihri, A.; Palacin, S.; Fontecave, M. *Science* **2009**, *326*, 1384−1387. (b) Liang, H.-W.; Brüller, S.; Dong, R. H.; Zhang, J.; Feng, X. L.; Müllen, K. *Nat. Commun.* **2015**, *6*, 7992−7999.

(24) Conway, B. E.; Tilak, B. V. *Electrochim. Acta* **2002**, *47*, 3571−3594.

(25) Yin, Y.; Han, J.; Zhang, Y.; Zhang, X.; Xu, P.; Yuan, Q.; Samad, L.; Wang, X.; Wang, Y.; Zhang, Z.; Zhang, P.; Cao, X.; Song, B.; Jin, S. *J. Am. Chem. Soc.* **2016**, *138*, 7965−7972.

(26) Cui, W.; Liu, Q.; Cheng, N.; Asiri, A. M.; Sun, X. *Chem. Commun.* **2014**, *50*, 9340−9342.

(27) (a) Wang, Q.; Zhou, Z.-Y.; Lai, Y.-J.; You, Y.; Liu, J.-G.; Wu, X.-L.; Terefe, E.; Chen, C.; Song, L.; Rauf, M.; Tian, N.; Sun, S.-G. *J. Am. Chem. Soc.* **2014**, *136*, 10882−10885. (b) Thorum, M. S.; Hankett, J. M.; Gewirth, A. A. *J. Phys. Chem. Lett.* **2011**, *2*, 295−298.

DOI: 10.1021/jacs.6b09351
J. Am. Chem. Soc. 2016, 138, 14546−14549